Chapter 8

Introduction to “Spatiotemporal Chaos …”

8.1 Preface

The development of tools for describing spatio-temporal chaos constitutes one of the biggest challenges of modern nonlinear science. The phase space of a spatio-temporal system is infinite-dimensional, and the behaviour and the analysis of the solutions is complicated. A variety of methods have been developed for low-dimensional systems, and the usual strategy is to try to apply these methods to extended systems. In our paper, we have tried to tackle the problem of spatio-temporal chaos by means of periodic orbit theory in the regime where the chaos in the system is very weak. The method is based on approximating the flow by selected spatio-temporal “patterns” (periodic orbits). We construct a method for finding these spatio-temporal periodic orbits, and use the theory of spectral determinants to compute the long-term averages of the flow.

8.1.1 Statement of the problem

We study the Kuramoto-Sivashinsky equation as a paradigm of a chaotic system:

$$u_t = (u^2)_x - u_{xx} - \nu u_{xxxx}. \tag{8.1}$$

We have chosen this equation mainly due to its popularity among the physics community. The subscripts x and t denote the partial derivatives with respect to the space variable x and time t, respectively, and $\nu > 0$ is a parameter. The solution $u(x,t)$ is assumed periodic $u(x,t) = u(x + 2\pi, t)$.

Sometimes, one rescales the x coordinate as $x \to \sqrt{\nu}x$, time as $t \to \nu t$ and the solution u as $u \to u/\sqrt{\nu}$ so that the coefficient ν in (8.1) is removed:

$$u_t = (u^2)_x - u_{xx} - u_{xxxx}. \tag{8.2}$$

In this case, the solution is defined on the interval $x \in [0, L]$ with $L = 2\pi/\sqrt{\nu}$. The solution is periodic with period L.

In what follows, we shall use formulation (8.1).

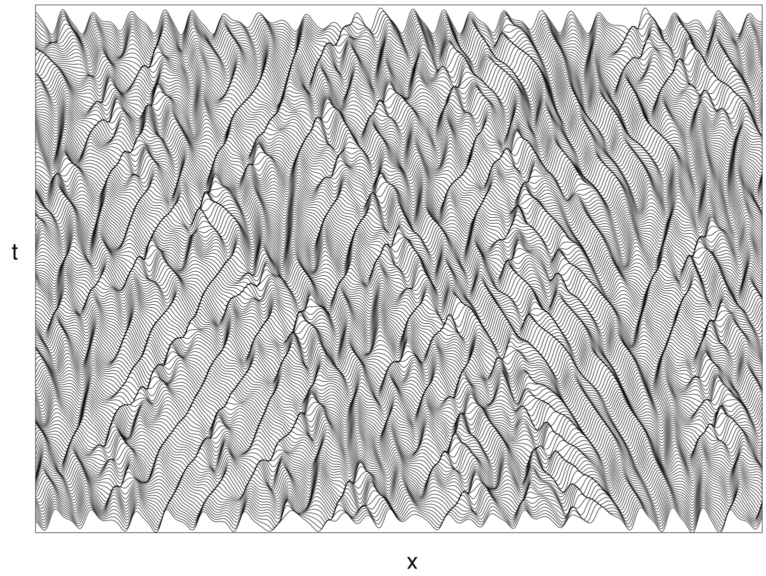

Figure 8.1: Solution of the model (8.2) $u(x,t)$ with $L = 1000$, courtesy of J. L. Hansen. The horizontal coordinate is x and the vertical is t. Only a part of the solution in the x direction is shown: the space variable x ranges from 100 to 300.

8.2 Intuititive periodic orbit theory

When one observes the solution of the system (8.2), presented in figure 8.1 one notices similar patterns in the shape of the function $u(x,t)$ when plotted versus x and t. Hills and valleys, some of them strongly resembling each other, move around and appear and disappear as time flows. One gets an impression that the function $u(x,t)$ approaches a series of patterns, then moves away from them while approaching another series of patterns, then after a while repeats some patterns it has encountered before (although not quite), and continuing in this way *ad infinitum*. There might be a hope that, after getting some experience, one can make a list of all the patterns which the solution of the system (8.1) tends to follow. These patterns will then be some functions $u_p(x,t)$. Since the patterns are repeated over and over, one might expect them to be periodic in time: $u_p(x,t+T_p) = u_p(x,t)$. These functions u_p will be exact (although unstable) *spatio-temporal periodic* solutions to the system (8.1).

We see that even though these solutions $u_p(x,t)$ are unstable, they are important for the dynamics. One knows that the periodic orbits fill up the attractor of the system. Thus, we can hope to predict the asymptotic properties of a solution to the system by averaging over the periodic patterns found, since the solution will always be close (at least partially) to some pattern. Each periodic pattern (orbit) will be assigned a weight dependent on the time an average solution spends close to the orbit. The more unstable the pattern $u_p(x,t)$ is, the less time a solution will spend close to it, thus the weight must depend on the stability of the orbit.

An exact version of these heuristic ideas will be derived later. We just want to give the reader a physical intuition of the meaning of the dry formulas of the following chapters will be.

8.3 Truncated system and its properties

8.3.1 Fourier expansion and its truncation

We expand equation (8.1) in a Fourier series

$$u(x,t) = \sum_{k=-\infty}^{+\infty} b_k(t)e^{ikx}, \tag{8.3}$$

and the resulting dynamics in Fourier space is:

$$\dot{b}_k = (k^2 - \nu k^4)b_k + ik\sum_{m=-\infty}^{+\infty} b_m b_{k-m}. \tag{8.4}$$

Since u is real, $b_k = b^*_{-k}$, where the star means the complex conjugate. We shall simplify the system (8.4) by putting $b_k = ia_k$, a_k being real. This corresponds to considering only the asymmetric solutions $u(x,t) = -u(-x,t)$. The system (8.4) becomes an infinite-dimensional system for *real* coefficient a_k:

$$\dot{a}_k = (k^2 - \nu k^4)a_k - k\sum_{m=-\infty}^{+\infty} a_m a_{k-m}, \tag{8.5}$$

with $a_k = -a_{-k}$. One can see that $\dot{a_0} = 0$, which corresponds to the conservation of the mean in equation (8.1)

$$\frac{d}{dt}\int u(x,t)\mathrm{d}x = 0.$$

For numerical treatment, we must truncate the system (8.5) by putting $a_k = 0$ if $k > N$. We shall thus call N the *truncation number.*

We can rewrite the system (8.5) in the general form

$$\dot{\boldsymbol{a}} = \boldsymbol{f}(\boldsymbol{a}). \tag{8.6}$$

Here a is an N-dimensional vector, t is time and $\boldsymbol{f}$ is a nonlinear function. If the initial conditions $\boldsymbol{a}(t=0) = \boldsymbol{a}_0$ are specified, the equation (8.6) can be solved for $\boldsymbol{a}(t)$, and we assume that a solution exists for all $t > 0$. We shall denote such a solution, starting at the point $\boldsymbol{a}$ at the moment t as $\boldsymbol{f}^t(\boldsymbol{a})$.

In what follows, we shall also consider a discrete analogue of (8.6):

$$\boldsymbol{a}_{n+1} = \boldsymbol{f}(\boldsymbol{a}_n). \tag{8.7}$$

After n iterates, a point $\boldsymbol{a}$ will be mapped into the point $\boldsymbol{a}_n$ under the action of the map (8.7). In what follows, we shall denote this image $\boldsymbol{a}_n$ of the point $\boldsymbol{a}$ as $\boldsymbol{f}^n\boldsymbol{a}$.

Suppose we want to compute the long-term averages of any vector quantity $\boldsymbol{q}(\boldsymbol{a})$ for the maps (8.7). We define the integrated quantity $\boldsymbol{Q}^n$ to be

$$\boldsymbol{Q}^n(\boldsymbol{a}) = \sum_0^n \boldsymbol{q}(\boldsymbol{f}^n(\boldsymbol{a})). \tag{8.8}$$

Suppose $\boldsymbol{q}$ has m components $q_1, q_2, \ldots, q_m$, then $\boldsymbol{Q}^n$ will have m components as well. Analogously, if we want to average a quantity $\boldsymbol{q}$ for flows, we can define the integrated average $\boldsymbol{Q}^t$ in a manner similar to (8.8):

$$\boldsymbol{Q}^t(\boldsymbol{a}) = \int_0^t \boldsymbol{q}(\boldsymbol{f}^t(\boldsymbol{a}))\mathrm{d}t. \tag{8.9}$$

The problem we shall be concerned with is the following: given system (8.6) or (8.7), compute the averages

$$<< \boldsymbol{q} >>= \lim_{t\to\infty} \frac{1}{t} \left\langle \boldsymbol{Q}^t \right\rangle \tag{8.10}$$

for the continuous system (8.6) and

$$<< \boldsymbol{q} >>= \lim_{n\to\infty} \frac{1}{n} \left\langle \boldsymbol{Q}^n \right\rangle \tag{8.11}$$

for the discrete system (8.7). Here $< \cdot >$ denotes a space average and $<< \cdot >>$ a space and time average.

For example, the Lyapunov exponents h_i, $i = 1, \ldots, n$ for discrete systems of the type (8.7) are defined as [2]

$$h_i = \lim_{n\to\infty} \frac{1}{n} \left\langle \log |\lambda_i(\boldsymbol{Df}^n)| \right\rangle, \tag{8.12}$$

$\boldsymbol{Df}^n$ is the Jacobi matrix of the transformation $\boldsymbol{f}^n$ and λ_i is the ith eigenvector of this matrix. Analogously, for the continuum system (8.6) the definition is

$$h_i = \lim_{t\to\infty} \frac{1}{n} \left\langle \log |\lambda_i(\boldsymbol{Df}^t)| \right\rangle. \tag{8.13}$$

We see that the definition of the Lyapunov exponents (8.12-8.13) is a particular case of (8.10) and (8.11) with

$$q_i(\boldsymbol{a}) = \lambda_i(\boldsymbol{Df}^t(\boldsymbol{a})). \tag{8.14}$$

8.4 Properties of the Kuramoto-Sivashinsky equation

8.4.1 Poincaré plane

We analyse the system (8.1) on the Poincaré plane $a_1 = 0$. We take the initial conditions for the system (8.5) to be on that plane and integrate until the solution of the system (8.5) reaches $a_1 = 0$ for the first time. This will give the transition map Θ. If in the initial moment we had $a_1 = 0$ and $\dot{a_1} > 0$, at the first intersection of the plane $a_1 = 0$ (which defines the map $\boldsymbol{\Theta}$) we must necessarily have $\dot{a}_1 < 0$. At the second intersection (which defines the map $\boldsymbol{\Theta}^2$) we shall have $\dot{a}_1 > 0$. Thus, if we are interested in computing the periodic orbits, we should define the Poincaré map $\boldsymbol{P}$ as $\boldsymbol{P} = \boldsymbol{\Theta}^2$, since the map $\boldsymbol{\Theta}$, as well as the map $\boldsymbol{\Theta}^{2n+1}$, cannot have any fixpoints for any integer n.

8.4.2 Symmetry reductions

One can see that the system (8.5) possesses a symmetry S (shift symmetry) defined as

$$\boldsymbol{S}u(x,t) = u(x+\pi, t),$$

which can be written in terms of the coefficients a_k in (8.5) as

$$\boldsymbol{S} : a_{2k} \to a_{2k}, a_{2k+1} \to -a_{2k+1}.$$

It is easy to see that $\boldsymbol{S}^2 = \boldsymbol{1}$.

The attractor $\mathcal{A}_{tot}$ of the system (8.5) can then be decomposed under the action of the maps $\boldsymbol{S}$ and $\boldsymbol{\Theta}$ (defined above) into four parts. The 'fundamental part' $\mathcal{A}$ has three images: $\boldsymbol{S}\mathcal{A}$, $\boldsymbol{S\Theta}\mathcal{A}$ and $\boldsymbol{\Theta S}\mathcal{A}$, and

$$\mathcal{A}_{tot} = \mathcal{A} \cup \boldsymbol{S}\mathcal{A} \cup \boldsymbol{S\Theta}\mathcal{A} \cup \boldsymbol{\Theta S}\mathcal{A}.$$

There are only four pieces, since $\boldsymbol{\Theta}^2 = \boldsymbol{P}$ and the attractor is invariant with respect to the Poincaré map $\boldsymbol{P}$. This symmetry reduction allows us to simplify the analysis of the system by considering only the 'fundamental part' of the attractor $\mathcal{A}$.

8.4.3 Transition to chaos

One observes that the trivial solution $u = 0$ is always a solution of the system (8.5). This trivial solution is stable if ν is sufficiently large. When ν is decreased, the system undergoes a series of bifurcation, studied, for example, in [3]. The bifurcation structure of the system is quite intricate and we shall not go into the details since this is of no particular interest to us. The Feigenbaum tree for the system when the parameter ν is changed is shown in our article [1] in Figure 1. The parameter values we shall work with are marked with arrows.

8.5 General theory of averages through periodic orbits

In this section, we shall outline the main premises and results of the periodic orbit theory and formalise the heuristic ideas described in section 2 of this chapter. What we are ultimately striving to do is to write the formulas for averages of the type (8.10) or (8.11), for example, the Lyapunov exponents, summing over periodic orbits. This will allow us to compute these averages without making long-term numerical simulations of the systems. If we assume that the picture of the flow following the pieces of "patterns" is correct, the more "patterns" we assemble, the more accurate our answer will be.

Unfortunately, the derivation of the method will be quite dry and technical. The reader concerned with the applications of the theory could go directly to the formula for the Fredholm determinant (8.49) below, take it for granted and follow the recommendations for using this expression immediately afterwards. In our derivation, we follow [4], chapter 5.

8.5.1 Perron-Frobenius operators

Suppose we sprinkle small weightless particles in the phase space of our dynamical system (8.6) or (8.7) and want to see how the density of those particles evolves in space and time. Suppose the particles are distributed initially with the density $\rho(\boldsymbol{a}, t = 0) = \rho_0(\boldsymbol{a})$. Under the action of the dynamical system, the particles move around, and the density $\rho(\boldsymbol{a}, t)$ changes to $\rho(\boldsymbol{a}, t) = \mathcal{L}^t\rho_0(\boldsymbol{a})$. We can define an evolution operator, which describes how the local particle density changes with respect to time:

$$\rho(\boldsymbol{a}, t) = \mathcal{L}^t\rho_0(\boldsymbol{a}) = \int \delta(\boldsymbol{a} - \boldsymbol{f}^t\boldsymbol{b})\rho_0(\boldsymbol{b})\mathrm{d}\boldsymbol{b}. \tag{8.15}$$

The integral is taken over the phase space. Here $\boldsymbol{f}^t\boldsymbol{b}$ is the solution of the differential equation (8.6) at time t starting the initial condition at $\boldsymbol{b}$ at $t = 0$.

If we add more particles to the initial flow, the new particles will float independently of the old ones. Thus the evolution operator $\mathcal{L}^t$ is linear:

$$\mathcal{L}^t(\rho_1(\boldsymbol{a}) + \rho_2(\boldsymbol{a})) = \mathcal{L}^t\rho_1(\boldsymbol{a}) + \mathcal{L}^t\rho_2(\boldsymbol{a}), \tag{8.16}$$

and, in a similar way,

$$\mathcal{L}^t(\alpha\rho_0(\boldsymbol{a})) = \alpha\mathcal{L}^t\rho_0(\boldsymbol{a}), \tag{8.17}$$

where α is an arbitrary constant. For the discrete case (8.7), the analogue of (8.15) is

$$\rho(\boldsymbol{a}, n) = \mathcal{L}^n\rho_0(\boldsymbol{a}) = \int \delta(\boldsymbol{a} - \boldsymbol{f}^n\boldsymbol{b})\rho_0(\boldsymbol{b})\mathrm{d}\boldsymbol{b}. \tag{8.18}$$

Here $\boldsymbol{f}^n$ is the nth iterate of the function $\boldsymbol{f}$ in (8.7). The linear operator $\mathcal{L}$ is the Perron-Frobenius operator for the map $\boldsymbol{f}$:

$$\mathcal{L}\rho_0(\boldsymbol{a}) = \int \delta(\boldsymbol{a} - \boldsymbol{f}\boldsymbol{b})\rho_0(\boldsymbol{b})\mathrm{d}\boldsymbol{b}. \tag{8.19}$$

Since $\mathcal{L}$ is a linear operator, its eigenvalues and eigenvectors can be found. We shall now show that these eigenvalues and eigenvectors have a definite physical meaning. Suppose that some particles can escape from the system. In this case, the largest (in the absolute value) eigenvalue λ_1 of $\mathcal{L}$ must be less than 1 (otherwise the density will grow exponentially). In the limit of large n, one can approximate the density of particles at the nth step with exponential accuracy as

$$\rho(\boldsymbol{a}, n) \simeq \lambda_1^n e_1(\boldsymbol{a}), \tag{8.20}$$

where $e_1(\boldsymbol{a})$ is the eigenvector corresponding to the eigenvalue λ_1. Note that an eigenvalue of a linear operator in this case is a *scalar* function, that is why we do not use the bold face notation for the eigenvectors.

Thus, the *decay rate* γ is equivalent to

$$\gamma = \lim_{n\to\infty} \log \frac{\|\rho_n\|}{\|\rho_0\|} = \log(\lambda_1). \tag{8.21}$$

When the density becomes sufficiently small, the remaining particles are distributed according to the eigenvector $e_1(\boldsymbol{a})$.

8.5.2 Generalised Perron-Frobenius operators

The generalised version of the Perron-Frobenius operator can be formulated, allowing us to compute the averages of the flow quantities $\boldsymbol{Q}$ in (8.10) and (8.11). First, we define the generating function for averages by means of the following linear operator:

$$\mathcal{L}_{\boldsymbol{\beta}}g(\boldsymbol{a}) = \int \delta(\boldsymbol{a} - \boldsymbol{f}\boldsymbol{b})\rho_0(\boldsymbol{b})e^{\boldsymbol{\beta}\cdot\boldsymbol{Q}(\boldsymbol{b})}g(\boldsymbol{b})\mathrm{d}\boldsymbol{b}, \tag{8.22}$$

where g is an arbitrary function, $\boldsymbol{\beta}$ is a (co)vector of the same dimension as $\boldsymbol{Q}$. The dot denotes the scalar product. The n-th iterate of the operator $\mathcal{L}_{\boldsymbol{\beta}}$ is

$$\mathcal{L}^n_{\boldsymbol{\beta}}g(\boldsymbol{a}) = \int \delta(\boldsymbol{a} - \boldsymbol{f}^n\boldsymbol{b})\rho_0(\boldsymbol{b})e^{\boldsymbol{\beta}\cdot\boldsymbol{Q}^n(\boldsymbol{b})}g(\boldsymbol{b})\mathrm{d}\boldsymbol{b}, \tag{8.23}$$

thus the operator $\mathcal{L}_{\boldsymbol{\beta}}$ is multiplicative along the flow. If $\boldsymbol{\beta} = 0$, $\mathcal{L}_{\boldsymbol{\beta}}$ is the usual Perron-Frobenius operator (8.19). We shall now show that the long-term averages of the flow can be computed using the eigenvalues of this generalised Perron-Frobenius operator (8.22).

Suppose $E(\boldsymbol{\beta})$ is the largest eigenvalue of the operator $\mathcal{L}_{\boldsymbol{\beta}}$, then the average growth of the function $e^{\boldsymbol{\beta}\cdot\boldsymbol{Q}}$ can be approximated for large n as

$$\left\langle e^{\boldsymbol{\beta}\cdot\boldsymbol{Q}^n}\right\rangle \simeq E(\boldsymbol{\beta})^n. \tag{8.24}$$

Here $<\cdot>$ denote a space average. From the definition of the averages (8.11), we have

$$<<\boldsymbol{q}>>= \lim_{n\to\infty}\frac{1}{n}\langle\boldsymbol{Q}^n\rangle = \frac{\partial\log(E(\boldsymbol{\beta}))}{\partial\boldsymbol{\beta}}\Big|_{\boldsymbol{\beta}=0}, \tag{8.25}$$

where $<<\cdot>>$ denotes a space and time average. We use the notation $\partial/\partial\boldsymbol{\beta}$, we hope that this notation is quite transparent. For example, equation (8.25) can be written explicitly for each component i as:

$$<<q_i>>= \lim_{n\to\infty}\frac{1}{n}\langle\boldsymbol{Q}^n\rangle = \frac{\partial\log(E(\boldsymbol{\beta}))}{\partial\beta_i}\Big|_{\boldsymbol{\beta}=0}. \tag{8.26}$$

Thus, we arrive at the fundamental formula connecting the averages of an observable $\boldsymbol{q}$ and the eigenvalue $E(\boldsymbol{\beta})$ of the operator $\mathcal{L}_{\boldsymbol{\beta}}$:

$$<<\boldsymbol{q}>>= \frac{\partial\log(E(\boldsymbol{\beta}))}{\partial\boldsymbol{\beta}}\Big|_{\boldsymbol{\beta}=0}. \tag{8.27}$$

It will be more convenient for us to work with the generating function of the averages, defined as:

$$s(\boldsymbol{\beta}) = \lim_{n\to\infty}\frac{1}{n}\log\left\langle e^{\boldsymbol{\beta}\cdot\boldsymbol{Q}^n}\right\rangle. \tag{8.28}$$

Then, differentiating $s(\boldsymbol{\beta})$ with respect to $\boldsymbol{\beta}$ and putting $\boldsymbol{\beta} = 0$, we observe that

$$<<\boldsymbol{q}>>= \lim_{n\to\infty}\frac{1}{n}\langle\boldsymbol{Q}^n\rangle = \frac{\partial s}{\partial\boldsymbol{\beta}}\Big|_{\boldsymbol{\beta}=0}. \tag{8.29}$$

Combining (8.25) and (8.29), we see that $s(\boldsymbol{\beta})$ is connected with the eigenvalue $E(\boldsymbol{\beta})$ by means of the following relationship:

$$s(\boldsymbol{\beta}) = \log E(\boldsymbol{\beta}). \tag{8.30}$$

We shall derive the formulas for explicit computation of $s(\boldsymbol{\beta})$ in (8.28), which is more practical than computing the eigenvalue $E(\boldsymbol{\beta})$.

For flows, the generalised Perron-Frobenius operator can be defined similarly to (8.22) as

$$\mathcal{L}^t_{\boldsymbol{\beta}}g(\boldsymbol{a}) = \int\delta(\boldsymbol{a}-\boldsymbol{f}^t\boldsymbol{b})e^{\boldsymbol{\beta}\cdot\boldsymbol{Q}^t}g(\boldsymbol{b})\mathrm{d}\boldsymbol{b}. \tag{8.31}$$

The generating function for the averages $s(\boldsymbol{\beta})$ is also defined similarly to (8.28):

$$s(\boldsymbol{\beta}) = \lim_{t\to\infty}\frac{1}{t}\log\left\langle e^{\boldsymbol{\beta}\cdot\boldsymbol{Q}^t}\right\rangle. \tag{8.32}$$

Then, completely analogously to the previous results, we get

$$<< \boldsymbol{q} >>= \lim_{t\to\infty} \frac{1}{t} \left\langle \boldsymbol{Q}^t \right\rangle = \frac{\partial s}{\partial \boldsymbol{\beta}} \Big|_{\boldsymbol{\beta}=0} . \tag{8.33}$$

The averages of the quantity $\boldsymbol{q}$ are now

$$<< \boldsymbol{q} >>= \lim_{t\to\infty} \frac{1}{t} \left\langle \boldsymbol{Q}^t \right\rangle = \frac{\partial s}{\partial \boldsymbol{\beta}} \Big|_{\boldsymbol{\beta}=0} . \tag{8.34}$$

The relationship (8.30) holds for flows as well.

In the next section we shall express $s(\boldsymbol{\beta})$ as a sum of periodic orbits, thus implementing our physical picture based on the flow moving along the “patterns”.

8.6 Periodic orbit expressions for averages

We shall first derive the formulas for the maps and afterwards give the corresponding expressions for the flows. The question which interests us is the computation of the quantity $\left\langle \mathcal{L}^n_{\boldsymbol{\beta}} \circ 1 \right\rangle$ (1 meaning the function equal to unity everywhere, and $\mathcal{L}_{\boldsymbol{\beta}}$ is defined as in (8.22)), which is the same as $\left\langle e^{\boldsymbol{\beta}\cdot\boldsymbol{Q}} \right\rangle$. Suppose, again, that $E(\boldsymbol{\beta})$ is the largest eigenvalue of $\mathcal{L}_{\boldsymbol{\beta}}$. Then, for large n, the operator $\mathcal{L}^n_{\boldsymbol{\beta}}$ applied to the unit function 1 grows as $E(\boldsymbol{\beta})^n$. It is easy to see that also $\mathrm{tr}\mathcal{L}^n_{\boldsymbol{\beta}}$ grows as $E(\boldsymbol{\beta})^n$, since $\mathrm{tr}\mathcal{L}^n_{\boldsymbol{\beta}}$ is a sum of eigenvalues of $\mathcal{L}^n_{\boldsymbol{\beta}}$. Thus, we can write approximately that for large n

$$\left\langle \mathcal{L}^n_{\boldsymbol{\beta}} \right\rangle \simeq \mathrm{tr}\mathcal{L}^n_{\boldsymbol{\beta}}. \tag{8.35}$$

On the other hand, the trace of the operator $\mathcal{L}_{\boldsymbol{\beta}}$ can be computed explicitly using the expression for integrating over the delta-functions [5]:

$$\int \delta(\boldsymbol{g}(\boldsymbol{a}))\boldsymbol{h}(\boldsymbol{a})\mathrm{d}\boldsymbol{a} = \sum_{\boldsymbol{a}_i:\boldsymbol{g}(\boldsymbol{a}_i)=0} \frac{h(\boldsymbol{a}_i)}{|\det(\boldsymbol{D}\boldsymbol{g}(\boldsymbol{a}_i))|}. \tag{8.36}$$

Here $\boldsymbol{g}$ and $\boldsymbol{h}$ are arbitrary vector-functions, $\mathbf{Dg}$ is the Jacobi matrix of the function g and the summation is performed over all the zeroes of the function g. Using the expression (8.36), the trace of the operator $\mathcal{L}^n_{\boldsymbol{\beta}}$ can be evaluated in terms of zeroes of the function $\boldsymbol{a} - f^n\boldsymbol{a}$:

$$\mathrm{tr}\mathcal{L}^n_{\boldsymbol{\beta}} = \int \delta(\boldsymbol{a} - \boldsymbol{f}^n(\boldsymbol{a}))e^{\boldsymbol{\beta}\cdot\boldsymbol{Q}(\boldsymbol{a})} = \sum_{\boldsymbol{a}_i:\boldsymbol{f}^n(\boldsymbol{a}_i)=\boldsymbol{a}_i} \frac{e^{\boldsymbol{\beta}\cdot\boldsymbol{Q}(\boldsymbol{a}_i)}}{\det|\mathbf{1} - \boldsymbol{D}\boldsymbol{f}^n(\boldsymbol{a}_i)|}. \tag{8.37}$$

The points $\boldsymbol{a}_i$ are such that the function f iterates them back to themselves after n iterates: $\boldsymbol{f}^n(\boldsymbol{a}_i) = \boldsymbol{a}_i$, and the summation is performed over all such points. These points can be divided into subgroups, as we shall illustrate for the particular example $n = 4$. All the points $\boldsymbol{a}_i$ for this example satisfy $\boldsymbol{f}^4(\boldsymbol{a}_i) = \boldsymbol{a}_i$. Some of these points $\boldsymbol{a}_i$ are fixed points, since $\boldsymbol{f}^4(\boldsymbol{a}_i) = \boldsymbol{a}_i$ if $\boldsymbol{f}(\boldsymbol{a}_i) = \boldsymbol{a}_i$. Some of these points are periodic points of length 2, satisfying $\boldsymbol{f}^2(\boldsymbol{a}_i) = \boldsymbol{a}_i$, since in this case we also have $\boldsymbol{f}^4(\boldsymbol{a}_i) = \boldsymbol{a}_i$. For each cycle of length 2, there will be 2 such points, since $\boldsymbol{a}_i$ and $\boldsymbol{f}\boldsymbol{a}_i$ are different, but both satisfy $\boldsymbol{f}^4(\boldsymbol{a}_i) = \boldsymbol{a}_i$ and $\boldsymbol{f}^4(f\boldsymbol{a}_i) = \boldsymbol{f}\boldsymbol{a}_i$. Finally, some of these points are cycles of length 4. For each cycle of length 4, there will be 4 different points, which are iterates of each other: $\boldsymbol{a}_i$, $\boldsymbol{f}\boldsymbol{a}_i$, $\boldsymbol{f}^2\boldsymbol{a}_i$ and $\boldsymbol{f}^3\boldsymbol{a}_i$. One can see that this classification completely exhausts all the points $\boldsymbol{a}_i$ such that $\boldsymbol{f}^4\boldsymbol{a}_i = \boldsymbol{a}_i$. Analogously, we can classify the solutions of the equation $\boldsymbol{f}^n\boldsymbol{a}_i = \boldsymbol{a}_i$ into classes of cycles which are cycles of the length n_p, where n_p is a divisor of n.

Finally, one can rewrite expression (8.37) as the sum over all *prime cycles* and their repeats. A prime cycle is a cycle which is not a repeat of a cycle of a lesser length. The length of such a cycle n_p will be a divisor of n: $n = n_p r$, r being an integer. Expression (8.37) then transforms to

$$\mathrm{tr}\mathcal{L}^n_{\boldsymbol{\beta}} = \sum_p n_p \sum_{r=0}^{\infty} \delta_{n,n_p r} \frac{e^{r\boldsymbol{\beta}\cdot\boldsymbol{Q}_p}}{\det|\mathbf{1} - \boldsymbol{J}_p^r|}. \tag{8.38}$$

Here the index p indicates the prime cycles, r is the number of the repeats of the prime cycle, $\boldsymbol{Q}_p$ is the value of the integral quantity $\boldsymbol{Q}$ from (8.8) along the cycle p, $\boldsymbol{J}_p$ is the Jacobi matrix of the mapping function f on the prime cycle, and $\delta_{n,n_p r}$ is the Kronecker delta.

It is easier to work not with trace (8.38) but with its discrete Laplace transform:

$$\mathrm{tr}\mathcal{L}_{\boldsymbol{\beta}}(s) = \sum_{n=1}^{\infty} e^{-ns}\mathrm{tr}\mathcal{L}^n_{\boldsymbol{\beta}} = \sum_p n_p \sum_{r=1}^{\infty} \frac{e^{-n_p r s} e^{r\boldsymbol{\beta}\cdot\boldsymbol{Q}_p}}{\det|\mathbf{1} - \boldsymbol{J}_p^r|}, \tag{8.39}$$

which can be rewritten as

$$\mathrm{tr}\mathcal{L}_{\boldsymbol{\beta}}(s) = \sum_{n=1}^{\infty} e^{-ns}\mathrm{tr}\mathcal{L}^n_{\boldsymbol{\beta}} = \mathrm{tr}\frac{e^{-s}\mathcal{L}_{\boldsymbol{\beta}}}{1 - e^{-s}\mathcal{L}_{\boldsymbol{\beta}}} = \sum_\alpha \frac{e^{-s}E_\alpha}{1 - e^{-s}E_\alpha} \tag{8.40}$$

where sum in equation (8.40) is taken over all the eigenvalues E_α of the operator $\mathcal{L}_{\boldsymbol{\beta}}$. Equation (8.40) follows directly from the definition of the trace and the expression for the geometric sum $\sum_{n=0}^{\infty} q^n = (1-q)^{-1}$. We see that the expression (8.40) for $\mathrm{tr}\mathcal{L}_{\boldsymbol{\beta}}(s)$ diverges whenever s approaches $\log E_\alpha$.

For flows, formulas analogous to (8.39-8.40) can be derived. We have

$$\mathrm{tr}\mathcal{L}^t_{\boldsymbol{\beta}} = \sum_p T_p \sum_{r=0}^{\infty} \delta(t - rT_p) \frac{e^{r\boldsymbol{\beta}\cdot\boldsymbol{Q}_p}}{\det|\mathbf{1} - \boldsymbol{J}_p^r|}, \tag{8.41}$$

where T_p is the period of the orbit p and $\boldsymbol{Q}_p$ is again the value of the integral quantity $\boldsymbol{Q}$ from (8.9) along the orbit p, and δ is the Dirac delta-function. A Laplace transform yields

$$\mathrm{tr}\mathcal{L}_{\boldsymbol{\beta}}(s) = \int_0^{\infty} e^{-st}\mathrm{tr}\mathcal{L}^t_{\boldsymbol{\beta}} = \sum_p T_p \sum_{r=1}^{\infty} \frac{e^{-r(sT_p + \boldsymbol{\beta}\cdot\boldsymbol{Q}_p)}}{\det|\mathbf{1} - \boldsymbol{J}_p^r|}. \tag{8.42}$$

If we denote the eigenvalues of $\mathcal{L}_{\boldsymbol{\beta}}$ as e^s_α, then $\mathrm{tr}\mathcal{L}_{\boldsymbol{\beta}} \sim e^{s_\alpha t}$ and instead of (8.40) we get:

$$\mathrm{tr}\mathcal{L}_{\boldsymbol{\beta}}(s) = \sum_\alpha \frac{1}{s - s_\alpha}. \tag{8.43}$$

Again, the trace diverges whenever s approaches the log of an eigenvalue.

Recall now the relationship between the averaged generating function $s(\boldsymbol{\beta})$ and the eigenvalue $E(\boldsymbol{\beta})$ given by (8.30): $s(\boldsymbol{\beta}) = \log E(\boldsymbol{\beta})$. We see that the poles of (8.40) and

(8.43) correspond precisely to the value of the generating function $s(\boldsymbol{\beta})$ given by (8.28) and (8.32). Thus, the problem of computing the generating function for the averages $s(\boldsymbol{\beta})$ is reduced to determining the poles of a function defined as a sum over periodic orbits. In principle, our problem is solved: we have expressed the desired averages in terms of periodic orbits. However, it is very inconvenient to look for the poles of a function in a complex plane. By going to *spectral determinants*, we can reduce the problem to the computation of *zeroes* of a function in a complex plane, which is computationally much easier.

8.6.1 Spectral determinants

As usual, we shall derive the formulas for the discrete systems first. The idea is to define the spectral determinant

$$F(z) = \det(1 - e^{-s}\mathcal{L}_{\boldsymbol{\beta}}) = \Pi_\alpha(1 - e^{-s}E_\alpha), \tag{8.44}$$

where E_α are the eigenvalues of the operator $\mathcal{L}_{\boldsymbol{\beta}}$. The eigenvalues of $\mathcal{L}_{\boldsymbol{\beta}}$ can then be obtained by searching for *zeroes* of the function $F(z)$, which is much more convenient than looking for the poles of the functions (8.40) or (8.43). Our goal will be to express (8.44) in terms of periodic orbits.

We use the following identity holding for any matrix M:

$$\log\det M = \operatorname{tr}\log M. \tag{8.45}$$

The identity (8.45) holds also when M is a linear operator of the *trace class*, i.e., $\operatorname{tr}M$ is bounded. We shall use (8.45) with $M = 1 - e^{-s}\mathcal{L}_{\boldsymbol{\beta}}$. First, we expand $\log(1 - e^{-s}\mathcal{L}_{\boldsymbol{\beta}})$:

$$\log(1 - e^{-s}\operatorname{tr}\mathcal{L}_{\boldsymbol{\beta}}) = \sum_{n=1}^{\infty}\frac{1}{n}e^{-ns}\mathcal{L}^n_{\boldsymbol{\beta}}. \tag{8.46}$$

Next, we exponentiate both sides of (8.45) and use (8.46) to get the expression for the spectral determinant $F(z)$:

$$F(z,\boldsymbol{\beta}) = \det(1 - e^{-s}\mathcal{L}_{\boldsymbol{\beta}}) = e^{-\sum\limits_{n_p}\sum\limits_{r=1}^{\infty}\frac{1}{r}\frac{e^{-n_p r s}e^{r\boldsymbol{\beta}\cdot\boldsymbol{Q}_p}}{\det|\mathbf{1}-\boldsymbol{J}_p^r|}}. \tag{8.47}$$

For flows, the expression for the spectral determinant is

$$F(s,\boldsymbol{\beta}) = \det(1 - s\mathcal{L}_{\boldsymbol{\beta}}) = e^{-\sum\limits_{n_p}\sum\limits_{r=1}^{\infty}\frac{1}{r}\frac{e^{r(-sT_p+\boldsymbol{\beta}\cdot\boldsymbol{Q}_p)}}{\det|\mathbf{1}-\boldsymbol{J}_p^r|}}. \tag{8.48}$$

One can consider a map as a particular case of the flow when all the periods T_p are equal to the length of the orbit $T_p = n_p$, which transforms (8.47) into (8.48).

Formulas (8.47) and (8.48) are the final expressions for the averages in terms of periodic orbits. Fixing $\boldsymbol{\beta}$, we can find the root(s) $s(\boldsymbol{\beta})$ satisfying $F(s(\boldsymbol{\beta}),\boldsymbol{\beta}) = 0$. Then, as mentioned before, $s(\boldsymbol{\beta})$ will be precisely the averaged generating function (8.28) or (8.32), and the averages can be computed by taking the derivatives of $s(\boldsymbol{\beta})$ according to (8.29) and (8.33).

8.6.2 Practical implementation of spectral determinants: recycling

We shall explain now how (8.48) was computed. This method for the computation is readily generalised for (8.47).

Formula (8.48), as it stands, is not very practical. This expression is an infinite sum, and easily get the wrong result by summing the terms in the wrong order. The idea of *recycling* is to sum the shortest cycles first. This way the convergence of the sum is optimal. This is also physical, since the shortest cycles play more important role in the dynamics than the long ones. We shall introduce an order parameter z into (8.48) and collect the coefficients with the same orders of z, putting $z = 1$ afterwards. We write

$$F(s, \boldsymbol{\beta}, z) = \det(1 - s\mathcal{L}_{\boldsymbol{\beta}}) = e^{-\sum_{n_p} \sum_{r=1}^{\infty} \frac{1}{r} \frac{z^{l_p r} e^{r(-sT_p + \boldsymbol{\beta} A_p)}}{\det |\mathbf{1} - \boldsymbol{J}_p^r|}} . \tag{8.49}$$

Cycles of length n_p, repeated r times, get a weight $z^{l_p r}$, where l_p is the topological length. By the topological length we mean, usually, the number of revolutions the orbit makes, i.e., $n_p = l_p$. (However, sometimes a different rule is desirable. An example of redefining the topological length is given in article [1] in section 4, when discussing the symbolic dynamics in the 3-cycle window).

It can be proven [6] that if the system is hyperbolic, (the Jacobians of the periodic orbits have eigenvalues isolated from 1) and the symbolic dynamics is complete, the Fredholm determinant (8.48) is an entire function of z in the complex plane. That means that if we expand $F(s, \boldsymbol{\beta}, z)$ in terms of z

$$F(s, \boldsymbol{\beta}, z) = \sum_{k \geq 0} c_k(s, \boldsymbol{\beta}) z^k, \tag{8.50}$$

the radius of convergence of the series (8.50) will be infinite, and the expansion coefficients c_k will decay faster than exponentially. If we truncate the series (8.50) after n terms, $F(s, \boldsymbol{\beta}, z)$ becomes a polynomial in z of the order n. According to (8.49), only periodic orbits of length less or equal to n have to be taken into account in order to compute the coefficients of this polynomial. The larger n is, the more accurate our result will be. If the terms c_k decay sufficiently fast, a small number of these coefficients will be needed, since the error we make by truncating the series (8.50) after n terms is of the order c_{n+1}. Thus, we have to use a few periodic orbits in order to approximate $F(s, \boldsymbol{\beta}, z)$ with the desired accuracy.

Our goal is to compute the coefficients $c_k(s, \boldsymbol{\beta})$ in (8.50) in terms of periodic orbits starting from (8.49). We shall now give an algorithm for doing it (which in itself is nothing more then expanding (8.49) in a Taylor series in z). We need to take the following steps:

1. Compute *all* periodic orbits up to given length n, their Jacobians and the contributions to the observables $\boldsymbol{Q}_p$ along the cycle. For example, for the Lyapunov exponents take $Q_{p,i} = \log |\lambda_i(\mathbf{J_p})|$, where λ_i is the i-th eigenvalue of the stability matrix $\mathbf{J_p}$ of the orbit p.

2. Compute the sum

$$S_n(z) = \sum_{n_p} \sum_{r=1}^{n} \frac{1}{r} \frac{z^{n_p r} e^{r(sT_p + \boldsymbol{\beta} \cdot \boldsymbol{Q}_p)}}{\det |\mathbf{1} - \boldsymbol{J}_p^r|} \tag{8.51}$$

as a polynomial in terms of z, i.e., determine the coefficients for z^k for $k = 1, \ldots, n$. Again, only the shortest periodic orbits with $n_p \leq n$ and r such that $rn_p \leq n$ have to be considered, since other terms will be of an order higher than z^n.

3. Compute $F(z)$ as

$$
\begin{aligned}
&F_n(s, \boldsymbol{\beta}, z) = e^{-S_n(z)} = \\
&1 - S_n(z) + \frac{S_n(z)^2}{2!} + \ldots (-1)^{n+1} \frac{S_n(z)^n}{n!}.
\end{aligned} \tag{8.52}
$$

When taking the k-th power of the polynomial $S_n(z)$, consider only terms up to order n. In this case, $F(z)$ will be a polynomial of order n in z, approximating $F(z)$.

4. Put $z = 1$ in $F_n(z)$ and obtain the function $F_n(s, \boldsymbol{\beta})$. For a fixed $\boldsymbol{\beta}$, find the zero of the function $s_n(\boldsymbol{\beta})$ satisfying $F_n(s_n(\boldsymbol{\beta}), \boldsymbol{\beta}) = 0$. Note that $s_n(0)$ is an approximation to the escape rate.

5. To compute the averages, calculate

$$
\frac{\partial s}{\partial \boldsymbol{\beta}} = -\frac{F_s}{F_{\boldsymbol{\beta}}}
$$

One can either do it numerically, since the function $s(\boldsymbol{\beta})$ is now known, or by cycle expansion of $F_{\boldsymbol{\beta}}$ and F_s. In the latter case, by differentiating (8.49) with respect to the parameters $\boldsymbol{\beta}$ and s, we get

$$
F_s = \sum_{r=1}^{\infty} T_p \frac{z^{n_p r} e^{r(sT_p + \boldsymbol{\beta} \boldsymbol{Q}_p)}}{\det |\mathbf{1} - \boldsymbol{J}_p^r|} F_n(z) = R_1(z) F_n(z)
$$

and

$$
F_{\boldsymbol{\beta}} = \sum_{r=1}^{\infty} \boldsymbol{Q}_p \frac{z^{n_p r} e^{r(sT_p + \boldsymbol{\beta} \cdot \boldsymbol{Q}_p)}}{\det |\mathbf{1} - \boldsymbol{J}_p^r|} F_n(z) = R_2(z) F_n(z),
$$

where R_1 and R_2 are polynomials of z of order n, and F_n is the n-th order truncation of (8.50). In the product $R_1 F_n$ and $R_2 F_n$ the terms of order higher than z^n must be neglected.

6. For a given n, we have obtained the decay rate $\gamma_n = s(\boldsymbol{\beta} = 0)$ and the average value of the observable

$$
<< \boldsymbol{q} >>= \frac{\partial s_n(\boldsymbol{\beta})}{\partial \boldsymbol{\beta}}.
$$

Increase n (if possible) and observe the convergence of the results with n.

8.6.3 Physical meaning of Fredholm determinants

The results above corroborate our physical picture of the possibility of describing the flow by "patterns". The expression (8.49) is a quantitative demonstration of our arguments about the solution following the parts of given patterns for some time, jumping to another "pattern" afterwards, etc. The vocabulary of the patterns is the collection of the *spatio-temporal* periodic orbits. The better our knowledge of this vocabulary, the higher an accuracy we can achieve in our computations. One can improve the knowledge of the vocabulary by increasing the number of patterns studied and investigating the rules for which patterns are admissible (pruning rules of the symbolic dynamics). The key problem is now *finding* the periodic orbits for the equation (8.5). Solving this problem is the main achievement of paper [1]. We shall describe our method below.

8.7 Difficulty of applying periodic orbit theory to high-dimensional systems

The major difficulty in applying the theory of cycle expansions to extended systems lies in the fact that *all* the periodic orbits up to a certain length have to be known. To accomplish this, we need to know the symbolic dynamics of the system. In the case when the flow or map is very high-dimensional, no general method for constructing the symbolic dynamics exists.

We study a relatively simple case when the dimension of the attractor does not exceed 2. The intersection of the attractor with the Poincaré plane $a_1 = 0$ (which has codimension 1) will then have a dimension less than 1, i.e., this intersection will be a line (or a subset of a line).

Even if the attractor is so low-dimensional, things are not that simple. We shall demonstrate this for the system (8.5). Projections of the solution onto different triples of coordinates are shown in article [1] in figure 2. We choose the Poincaré plane $a_1 = 0$, and plot the return map $a_6' = P_6(a_6)$ versus a_6 in figure 3 in the article, P_6 being the projection of the image of a point by the Poincaré map $\boldsymbol{P}$ on the 6-th coordinate. The graph of this map is a line. If this line was such that each preimage a_6 corresponded to one image a_6', then the problem would have been solved. The major obstacle in our way is a multi-valuededness of the return map. Indeed, since the return map $a_6 \to a_6'$ is a projection from an $(N-1)^2$ dimensional space onto a 2-dimensional space, it is not one-to-one, (some preimages a_6 have more than one image a_6'), and this will generally be the case for any extended system. We see that even if the chaos is weak and the dimension of the attractor is small, describing the dynamics is not so easy.

We shall get around this obstacle by finding a suitable parametrisation of the attractor. In fact, on the hyperplane $a_1 = 0$ in the phase space the attractor is just a 1-dimensional line, and the Poincaré map $(a_2, \ldots, n) \to \boldsymbol{P}(a_2', \ldots, a_n')$ is one-to-one. We parametrise the attractor $a_2 = a_2(s), a_3 = a_3(s), \ldots, a_N = a_N(s)$, where $s \in [s_l, s_r]$ is the parameter along the line. In this case, the Poincaré map can be written parametrically as

$$(a_2(s), \ldots, a_N(s)) \to \boldsymbol{P}(a_2(s), \ldots, a_N(s))$$

Since the attractor is invariant under the action of the map P, for each $s \in [s_l, s_r]$ the point $\boldsymbol{P}(a_2(s), \ldots, a_N(s))$ is an image of a point on the attractor. Hence, we can find a number $f(s)$ such that

$$(a_2(f(s)),\ldots,a_N(f(s))) = \boldsymbol{P}(a_2(s),\ldots,a_N(s)).$$

Instead of considering the $N-1$-dimensional map in the hyperplane $a_1 = 0$, we can consider a parametric one-dimensional map $s \to f(s)$ on the interval $s \in [s_l, s_r]$. For one-dimensional maps, a symbolic dynamics can be constructed and *all* periodic orbits up to the desired length can be found.

8.7.1 Parametrisation by periodic orbits

Suppose we have found a few periodic orbits. Some short periodic orbits can be found by random shooting. For each periodic orbit p of topological length l, we compute the corresponding periodic points $\boldsymbol{a}_p^1, \boldsymbol{a}_p^2, \ldots, \boldsymbol{a}_p^n$, where $\boldsymbol{a}_p = (a_1 = 0, a_2, \ldots, a_N)$ is a point on the Poincare plane. These periodic points satisfy:

$$\begin{aligned}
&\boldsymbol{P}(\boldsymbol{a}_p^1) = \boldsymbol{a}_p^2\\
&\boldsymbol{P}(\boldsymbol{a}_p^2) = \boldsymbol{a}_p^3\\
&\quad\ldots\\
&\boldsymbol{P}(\boldsymbol{a}_p^l) = \boldsymbol{a}_p^1.
\end{aligned} \tag{8.53}$$

We make a union of all the periodic points available:

$$\mathcal{Z} = \cup_p \cup_{l=1,\ldots,n_p} \left\{\boldsymbol{a}_p^l\right\}, \tag{8.54}$$

We want to enumerate the set of points of $\mathcal{Z}$ in the order they lie on the attractor. To do that, we plot all the periodic points on the return map $a_6 \to a_6'$ and look for the point which is closest to the end of the attractor. This point is assigned the number 1. The point from the set $\mathcal{Z}$ which is closest to the point number 1 is assigned number 2, and the point which is closest to number i and has not been enumerated yet is assigned the number $i+1$. Thus, we get the sequence of periodic points $\boldsymbol{a}^1, \ldots, \boldsymbol{a}^K$, where K is the total number of periodic points.

With the elements of $\mathcal{Z}$ in (8.54) thus enumerated, we can construct the approximate parametrisation s along the attractor. For the first point, we assign $s_1 = 0$. For the second point, $s_2 = \|\boldsymbol{a}^2 - \boldsymbol{a}^1\|$, where the norm is taken in the full Euclidean space. Similarly, $s_{i+1} = s_i + \|\boldsymbol{a}^{i+1} - \boldsymbol{a}^i\|$. Thus, each point i gets assigned the value of the parameter s_i.

The final step is to construct the map $s \to f(s)$. Since each point $\boldsymbol{a}^i$ in the set $\mathcal{Z}$ is a periodic point, under the action of the map P the points $\boldsymbol{a}^i$ are shuffled according to (8.53), but their union is still $\mathcal{Z}$ as given by (8.54). Thus, the set $\mathcal{Z}$ is invariant with respect to the Poincaré mapping $\boldsymbol{P} : \boldsymbol{P}(\mathcal{Z}) = \mathcal{Z}$.

Suppose the point number i from the set $\mathcal{Z}$ moves into the point number $j(i)$ under the action of the map P. Then, it is natural to define the desired parametric map $f(s)$ as

$$f(s_i) = s_{j(i)}. \tag{8.55}$$

We plot $f(s_i)$ versus s_i in [1] in figure 4 and observe that the resulting picture is a one-hump map. The symbolic dynamics has two symbols, 0 and 1. We call 0 the interval where $f(s)$ is an increasing function of s, and 1 the interval where $f(s)$ is a decreasing function of s. Then, any periodic point can be assigned a finite sequence of 0's and 1's. Not every finite sequence of 0 and 1 corresponds to a cycle though, since some symbolic sequences are forbidden (pruning).

Using this symbolic dynamics, all periodic orbits up to a desired length for the parametric map $s \to f(s)$ can be found. These periodic points s_p, corresponding to the given periodic orbits for the map $s \to f(s)$, can now be mapped onto the real space coordinates: $a_1 = 0, a_2(s_p), \ldots, a_N(s_p)$. The vector $a_1 = 0, a_2(s_p), \ldots, a_N(s_p)$ can now be used as an initial condition for the Newton iteration for finding periodic solutions in the full space. To find a periodic orbit in the full phase space, we need to solve N nonlinear equations (as usual, N is the dimension of the phase space):

$$\begin{aligned} & a_1(t = T_p) = 0 \\ & a_i(t = T_p) = a_i(t = 0), 2 \le i \le N, \end{aligned} \tag{8.56}$$

where $a_i(t)$ are the solutions of (8.5). The unknowns in (8.56) are the $N - 1$ initial conditions $a_2, \ldots, a_N$ and the period T_p. The resulting Newton iteration always converges. After the periodic orbit is found, its stability can be determined, and the spectral determinants can be applied to get expressions for the Lyapunov exponents. The resulting data are then compared to the Lyapunov exponents obtained by direct numerical simulation of (8.5). We find that they are in reasonable agreement.

Once these additional periodic orbits are found, more points can be added to the periodic points set $\mathcal{Z}$, and the numerical approximation to the map $s \to f(s)$ can be refined. If the number of points is sufficiently large, the transverse structure of the attractor shows up (see [1], Figure 4). Further refining has to incorporate the two-dimensionality of the mapping. In the future, we would like to generalise our methods to describe this two-dimensionality.

8.8 Conclusions

8.8.1 Power of periodic orbit theory

There is one fundamental question of the theory of extended systems we would like to raise now. We see from figure 1 of article [1] that the chaotic regions are mixed with the periodic windows. This is a general property of the transition to chaos of most chaotic systems. When computing averages by simulating equation (8.5) on a computer, one has to chose a finite truncation for the number of modes N. Analogously, simulating equation (8.1) on a computer by the finite-difference method requires taking a finite number of points on the lattice. Ideally, one would like N to tend to infinity, and expect a convergence of the desired average to some limiting value when $t \to \infty$. However, when changing N to $N+1$, one introduces a small perturbation to the original system, and there is a high probability that the system will end up in a different periodic window. Thus, there is no reason to expect nice behaviour of the computed averages when $N \to \infty$!

One could argue that the transition time increases dramatically when N is increased. In fact, if the solution is in a periodic window, but the stability of the corresponding stable cycle is very close to 1, a lot of time is required for the system to collapse to the stable cycle. In the limit $N \to \infty$, these transition times are so large that they are undetectable on a computer (due to numerical noise, for example), so this problem might not be so important *practically*. However, we feel that *theoretically* this problem is quite important, and an adequate answer is provided by the periodic orbit theory.

When a stable cycle is present, the limit $N \to \infty$ poses no ideological difficulties, since a stable cycle remains stable for small perturbations of the system. Thus, we also perform our periodic orbit calculations on the *repeller*, i.e the closure of the set of all the *unstable* periodic orbits. The usual methods fail in this case, since the motion collapses to the stable cycle and no information about the repeller can be extracted. In contrast, periodic orbit theory works even better here than for the chaotic case, since the complete grammar for the symbolic dynamics is known, and the convergence of the correspondence series is improved, (see Figure 10 and Table 2 of the article).

Other applications of periodic orbit theory are possible. One can, for example, compute the escape rate from the repeller to the limit cycle, which is an important physical quantity, estimating how fast the motion collapses to the stable cycle (this is done in Table 8.3 and Table 8.6, see below).

Besides allowing one to perform the computation of the repeller, periodic orbit theory enables one to derive estimates for quantities such as transition probabilities between different pieces of the attractor (say, $\mathcal{A}$ and $\Theta\mathcal{A}$). We have not done this since it seems to lack any physical motivation.

8.8.2 Deficiencies of the periodic orbit theory

The main drawback of periodic orbit theory is the requirement that *all* the periodic orbits up to a certain length and the symbolic dynamics are known. When the dimension of the attractor is large, no methods for computing the symbolic dynamics are known, and we are afraid that application of the periodic orbit theory to spatially extended systems will be stalled in the future by this great obstacle.

Even if the symbolic dynamics is known, obtaining the periodic orbits is a non-trivial computational task. To compute all periodic orbits for the system (8.5) up to the topological length 10, approximately 24 hours of CPU time on a DEC-Alpha station were needed. A direct numerical computation of the Lyapunov exponents with the same accuracy took considerably less time. Thus, if one can use the direct method, it is computationally more economical to do so. On the other hand, once the periodic orbits are computed, a great variety of averages can be obtained, thus making them useful for a deeper understanding of the underlying structure of the phase space.

Bibliography

[1] Christiansen, F., Cvitanović, P. & Putkaradze, V., (1997) *Spatiotemporal chaos in terms of unstable recurrent patterns*, *Nonlinearity*, **10**, *1*, 55.

[2] Ott, E. (1993) *Chaos in dynamical systems*, *Cambridge Univ. Press.*

[3] Kevrekidis, I. G., Nicolaenko B. & Scovel, J. C.,(1990) *"Back in the saddle again: a computer assisted study of the Kuramoto-Sivashinsky equation*, *SIAM J. Applied Math.* **50**, 760.

[4] Cvitanović, P., *Classical and quantum chaos*, in preparation.

[5] Vladimirov, V. S., (1981) *Equations of mathematical physics*, MIR, Moscow.

[6] Rugh, H. H., (1992) *Ph. D. Thesis*, *Copenhagen University.*

A Guide to Using Our Programs and Data Files.

This project required some extensive computer work and resulted in quite an amount of fortran programs and data files. We shall be happy if anyone could make use of our fortran codes for the sake of application to their specific problems or just for checking our results. All the program, data and tex files are available through the Internet. Check
http://WWW.nbi.dk/~ronnie/QCcourse/.

The figures showing the Feigenbaum trees (analogous to Figure 1 in [1], but for different N) are not included due to their size. A postscript version of the pictures takes several megabytes. At the same http address, you can obtain the gif version of the figures (they are much smaller than the postscript files but cannot be included in the tex file). Also, the data files and the fortran programs can be downloaded from the same site in the compressed form. All the data files have names which are self-explanatory. For example, if a file is called something16.3window.dat, it corresponds to $N = 16$ dimensions, 3-window case. If a file is called something16.chaotic.dat, it corresponds to the same system, but the chaotic regime. Hence, we write files as file**name**, where **name** can be equal to 9.chaotic.dat, 16.chaotic.dat, 17.chaotic.dat, 9.3window.dat or 16.3window.dat.

Data files available:

- Periodic orbit data (stability, period, etc.) are written in the file cyc**name**. The structure of the file is shown in table 8.1.
- Escape rate γ is written into the files zero**name**.
- All N Lyapunov exponents can be found in the files lyapfredh**name**.

Table 8.1: The structure of the data file cyc**name**

l	s_1	$\dots$	s_l	Topological length l and symbolic sequence
y_2^1	$\dots$	y_N^1		
	$\dots$			l Periodic points for the given orbit
y_2^l	$\dots$	y_N^l		
		T		Period of the orbit
		Λ_1		
		$\dots$		Stability coefficients
		Λ_N		

- The values of the coefficients of the Fredholm determinant are in coeff**name**. NB: These data do not exist for all cases.
- Values of the Fredholm determinant $F(s,0)$ as a function of s are in values**name**.
- The periodic orbit data contained in the files cyc**name**. Given that the dimension of the phase space is N, the structure of the data file is represented in the table 8.1.

Fortran programs available on the same http address in the compressed form. The following programs are included:

- fredholm.f

  Performs computation of the Fredholm determinant and Lyapunov exponents. Reads from the file cyc**name** and writes into the files zero**name**, values**name**, lyapfredh**name** and coeff**name** (optional). Requires NAG library (root-finding).

- makeparametric.f.

  Constructs the parametric map $s \to f(s)$ and the time ceiling function $T(s)$. Reads from the file cyc**name** and writes into the file parametric.dat. Requires NAG (Runge-Kutta integrator) to compute the return times.

- returnmap.f

  Computes the return map (Figure 3 in the article) for the given coordinate (parameter icoord in the program). Writes into the file returnmap.dat. Requires NAG (Runge-Kutta integrator).

- kscyc.f

  Computes periodic orbits, their stability and period by the method of Newton iteration (requires NAG: multi-dimensional root-finding and eigenvalues of a matrix).

Table 8.2: The numerical value of the escape rate γ and the first 4 lyapunov exponents estimated by means of periodic orbits for the 9-dimensional model, chaotic regime $\nu = 0.0351$.

l_{trunc}	γ	λ_1	λ_3	λ_4	λ_5
1	0.181405	1.197352	-5.935830	-8.615104	-11.543370
2	0.098903	0.975051	-6.261924	-8.546853	-11.225601
3	-0.016672	0.866897	-6.295820	-8.411136	-11.200248
4	0.343190	1.366972	-5.636953	-8.606413	-11.902256
5	0.037279	0.835898	-6.314786	-8.153886	-8.925157
6	0.006908	0.789140	-6.349519	-7.319485	-8.146655
7	0.010525	0.759081	-5.888360	-6.473228	-6.954056
8	0.018199	0.767811	-5.165383	-5.428893	-5.791945
9	0.016329	0.765077	-4.572622	-4.880796	-5.083030
10	0.010045	0.763972	-4.291482	-4.574804	-4.810942

- makeprofile.f

  Computes the transforms of the periodic orbits in real space. Optionally, it can calculate the differences between the periodic orbits. Reads from the file cyc**name** and writes into the file diff.dat. Requires NAG (Runge-Kutta integrator).

Please feel free to e-mail any comments, corrections or errors in the programs to putkarad@alf.nbi.dk

Results not included in [1]

To give We have not used all the results obtained by us in the article [1]. Equation (8.5) was solved with the number of modes $N = 9$, $N = 15$, $N = 16$, $N = 17$. We have only included the results for $N = 16$, since all the other cases are qualitatively (and ideologically) analogous to the case $N = 16$, but the precise values of escape rate and Lyapunov exponents are, of course, different. Below, we shall list the results for all cases for which the computations were made.

Table 8.3: The numerical value of the escape rate γ and the first 4 lyapunov exponents estimated by means of periodic orbits for the 9-dimensional model, period 3 window $\nu = 0.035143$.

l_{trunc}	γ	λ_1	λ_3	λ_4	λ_5
1	0.451491	0.749850	-6.477775	-8.456763	-11.026469
2	-0.190957	0.503207	-6.440229	-8.164360	-11.062223
3	-0.051202	0.547829	-6.445732	-8.227591	-10.496759
5	0.070897	0.726250	-4.825376	-3.251941	-1.528022
6	0.048679	0.630586	-4.367791	-4.386776	-4.753490
7	0.051899	0.640185	-3.086124	-3.438693	-3.771553
8	0.052376	0.644084	-2.629732	-2.707472	-2.805715
9	0.052311	0.642553	-2.509682	-2.597225	-2.678631

Table 8.4: The numerical value of the escape rate γ and the first 4 lyapunov exponents estimated by means of periodic orbits for the 15-dimensional model, chaotic regime $\nu = 0.0299$.

l_{trunc}	γ	λ_1	λ_3	λ_4	λ_5
1	0.292439	1.095381	-6.219602	-7.640735	-11.665645
2	0.096693	0.865384	-5.920297	-8.457884	-11.731865
3	-0.081454	0.691234	-5.771019	-8.375439	-11.692909
4	0.145159	0.437094	-5.422942	-9.403716	-9.934362
5	-0.002423	0.684319	-5.752819	-7.542551	-8.233828
6	0.039664	0.641756	-5.574065	-6.866960	-7.404961
7	0.012189	0.664374	-5.074519	-5.750664	-6.328097
8	0.002039	0.625057	-4.400768	-4.743388	-5.067439
9	0.012789	0.644544	-3.947124	-4.354239	-4.576697
10	0.019117	0.644538	-3.378577	-3.711215	-3.826372

Table 8.5: The numerical value of the escape rate γ and the first 4 lyapunov exponents estimated by means of periodic orbits for the 16-dimensional model, chaotic regime $\nu = 0.02991$.

l_{trunc}	γ	λ_1	λ_3	λ_4	λ_5
2	0.441948	0.981267	-6.087670	-7.846201	-11.685989
3	0.080117	0.765050	-5.853356	-8.148352	-11.681406
4	0.148583	0.703072	-5.751667	-8.529649	-11.105467
5	0.068513	0.727498	-5.785654	-7.786317	-9.171169
6	0.027724	0.699907	-5.708753	-7.028455	-8.132920
7	0.035137	0.693852	-5.383199	-6.371041	-7.152474
8	0.007104	0.675529	-4.823215	-5.445724	-6.008138
9	0.021066	0.673144	-4.338065	-4.818750	-5.079791
10	0.007367	0.646233	-4.032127	-4.437109	-4.778408

Table 8.6: The numerical value of the escape rate γ and the first 4 lyapunov exponents estimated by means of periodic orbits for the 16-dimensional model, period 3 window $\nu = 0.029924$. Fredholm determinant has no real roots when the orbits up to length $l_{trunc} = 4$ are summed.

l_{trunc}	γ	λ_1	λ_3	λ_4	λ_5
1	0.428143	0.703010	-5.703845	-8.845440	-11.771280
2	-0.187882	0.430485	-5.476388	-8.565405	-11.733163
3	-0.049325	0.469350	-5.512144	-8.388855	-10.681306
5	1.072468	0.585506	-5.597516	-8.811675	-12.204371
6	0.078008	0.547005	-4.544588	-5.921855	-7.360153
7	0.088132	0.598977	-1.663224	-2.590075	-2.429978
8	0.090425	0.631551	-1.074779	-1.105328	-1.022284
9	0.090101	0.618160	-1.591520	-1.541432	-1.806356
10	0.090065	0.621271	-1.333804	-1.404427	-1.484722

Table 8.7: The numerical value of the escape rate γ and the first 4 lyapunov exponents estimated by means of periodic orbits for the 17-dimensional model, chaotic regime $\nu = 0.02992$. No real root exists for $l_{trunc} = 8$.

l_{trunc}	γ	λ_1	λ_3	λ_4	λ_5
1	0.274182	1.079892	-6.184859	-7.618852	-11.674000
2	0.074540	0.851952	-5.872574	-8.415472	-11.736321
3	-0.159598	0.600268	-5.641082	-8.361154	-11.739655
4	0.086237	0.382140	-5.322086	-9.470242	-10.167605
5	-0.149015	0.502057	-5.533295	-7.704699	-8.588309
6	-0.080329	0.484562	-5.451683	-7.209586	-8.102709
7	-0.025821	0.490689	-4.946674	-5.538847	-5.684868
9	-0.013291	0.582015	-3.425984	-3.308398	-3.295470
10	-0.021366	0.484201	-2.982581	-3.127658	-3.478002